

DIMITRA paediatric skull phantoms: development of age-specific
paediatric models for dentomaxillofacial radiology research

Peer-reviewed author version

Oenning, Anne Caroline; Salmon, Benjamin; Vasconcelos, Karla de Faria; Nicolielo, Laura Ferreira Pinheiro; LAMBRICHTS, Ivo; Sanderink, Gerard; Pauwels, Ruben & Jacobs, Reinhilde (2018) DIMITRA paediatric skull phantoms: development of age-specific paediatric models for dentomaxillofacial radiology research. In: DENTOMAXILLOFACIAL RADIOLOGY, 47(3) (Art N° 20170285).

DOI: 10.1259/dmfr.20170285

Handle: <http://hdl.handle.net/1942/26560>

DIMITRA PEDIATRIC SKULL PHANTOMS: DEVELOPMENT OF AGE-SPECIFIC PEDIATRIC MODELS FOR DENTOMAXILLOFACIAL RADIOLOGY RESEARCH

Running Title: DIMITRA pediatric phantoms for dentomaxillofacial radiology research

Type of Manuscript: Technical report

Anne Caroline OENNING^{1,2*}, Benjamin SALMON^{1*}, Karla de Faria VASCONCELOS^{2,3}, Laura NICOLIELO³, Ivo LAMBRICHTS⁴, Gerard SANDERINK⁵, Ruben PAUWELS^{3,6}, DIMITRA group⁷, Reinhilde JACOBS^{3,8}.

¹EA2496, Orofacial Pathologies, Imaging and Biotherapies, Dental School Paris Descartes University, Sorbonne Paris Cité, France and Department of Odontology, AP-HP, Nord Val de Seine Hospital (Bretonneau), France.

²Department of Oral Diagnosis, Division of Oral Radiology, Piracicaba Dental School, University of Campinas (UNICAMP), Piracicaba, Sao Paulo, Brazil.

³OMFS IMPATH research group, Department of Imaging and Pathology, Faculty of Medicine, University of Leuven and Oral & Maxillofacial Surgery, University Hospitals Leuven, Leuven, Belgium.

⁴Morphology Group, Biomedical Research Institute, Hasselt University, Agoralaan Building C, Diepenbeek, Belgium.

⁵Department of Oral Radiology, Academic Center for Dentistry Amsterdam, University of Amsterdam and Vrije Universiteit, Amsterdam, The Netherlands.

⁶Department of Radiology, Faculty of Dentistry, Chulalongkorn University, Bangkok, Thailand.

⁷DIMITRA group available at www.dimitra.be

⁸Department of Dental Medicine, Karolinska Institutet, Stockholm, Sweden.

* These authors contributed equally to this work

Funding: The research leading to these results has received funding from the European Atomic Energy Community's Seventh Framework Programme FP7/2007–2011 under grant agreement no 604984 (OPERRA: Open Project for the European Radiation Research Area).

1
2
3
4
5
6
7
8
9
10
11
12
13
14
15
16
17
18
19
20
21
22
23
24
25
26
27
28
29
30
31
32
33
34
35
36
37
38
39
40
41
42
43
44
45
46
47
48
49
50
51
52
53
54
55
56
57
58
59
60
61
62
63
64
65

**DIMITRA PEDIATRIC SKULL PHANTOMS: DEVELOPMENT OF AGE-SPECIFIC
PEDIATRIC MODELS FOR DENTOMAXILLOFACIAL RADIOLOGY RESEARCH**

DMFR UNCORRECTED PROOFS

1
2
3
4 **ABSTRACT**
5

6
7 **Objectives:** This report aims to describe the development of age-specific phantoms for use in
8
9 pediatric dentomaxillofacial radiology research. These phantoms are denoted DIMITRA
10
11 pediatric skull phantoms as these have been primarily developed and validated for the DIMITRA
12
13 European research project (*Dentomaxillofacial paediatric imaging: an investigation towards low*
14
15 *dose radiation induced risks*).
16
17

18
19
20 **Methods:** To create the DIMITRA pediatric phantoms, six human pediatric skulls with estimated
21
22 ages ranging between 4 – 10 years old were selected, protected with non-radiopaque tape and
23
24 immersed in melted Mix-D soft tissue equivalent material, by means of a careful procedure
25
26 (layer-by- layer). Mandibles were immersed separately and a Mix-D tongue model was also
27
28 created. For validation purposes, the resulting pediatric phantoms were scanned using a cone-
29
30 beam CT unit with different exposure parameter settings.
31
32

33
34
35 **Results:** Preliminary images deriving from all scans were evaluated by two dentomaxillofacial
36
37 radiologists, to check for air bubbles, artefacts and inhomogeneities of the Mix-D and a
38
39 potential effect on the visualization of the jaw bone. Only skulls presenting perfect alignment of
40
41 Mix-D surrounding the bone surfaces with adequate and realistic soft tissue thickness density
42
43 were accepted.
44
45

46
47
48 **Conclusions:** The DIMITRA anthropomorphic phantoms can yield clinically equivalent images for
49
50 optimization studies in dentomaxillofacial research. In addition, the layer-by-layer technique
51
52 proved to be practical and reproducible, as long as recommendations are carefully followed.
53
54

55
56 **Key words:** cone-beam computed tomography; pediatric dentistry; radiation protection;
57
58 imaging phantoms
59
60
61
62
63
64
65

Introduction

It is well known that for each specific cone-beam CT (CBCT) scan, the exposure protocol should ideally consider both patient-specific features and indication-oriented requirements in order to obtain dose reduction at a satisfactory image quality level based on ALADA (As low as diagnostically acceptable)¹ and ALADAIP (As Low as Diagnostically Acceptable being Indication-oriented and Patient-specific).² Considering the large variety of technical parameters available on each CBCT device, suitable protocols should become more specific and controlled, and not only restricted to the manufacturer's default settings. For this purpose, optimization studies are needed combining patient factors, image quality and related acceptable dose levels in controlled settings. This is a true challenge requiring well-defined anthropomorphic phantoms, surely when it comes to pediatric protocol optimization.

A potential anthropomorphic phantom should contain materials that scatter and absorb ionizing radiation in a similar way to human tissues. Furthermore, the material should not only accurately mimic soft tissues without artefacts, yet also be universally available and reproducible.³ Commercially available phantoms made with tissue equivalent materials have been used as patient substitute during *in vitro* studies.⁴ In addition, distinct materials such as water, wax, resin, paraffin and polyethylene have been proposed,⁵⁻⁸ yet those materials have not been validated and/or compared when it comes to CBCT image quality studies. Amongst them, wax and water were most often used in research with CBCT.⁹⁻¹²

Human soft tissues, water and Mix-D (a mixture of paraffin wax and other chemicals) are able to yield similar x-ray transmission data, considering the very similar effective atomic number (*i.e.* soft tissues: 7.33, water: 7.42, Mix-D: 7.47).⁷ However, the volume of water surrounding

1
2
3
4 the anatomic sample is difficult to control and model following a natural soft tissue contour,
5
6 especially when different sizes of mandibles or skulls are scanned. This fact can bias the
7
8 experiment, producing unrealistic images that do not represent the quality of clinical scans due
9
10 to differences in attenuation, scatter and beam hardening. Moreover, some factors (e.g. noise
11
12 pattern, gray-scale) can change according the amount of tissue inside and outside the field of
13
14 view (FOV) in CBCT.^{13,14} In addition, anthropomorphic phantoms dedicated to radiographic
15
16 training of dental students do not produce satisfactory CBCT scans for image quality
17
18 assessment, and currently, only adult phantoms are available.
19
20
21
22
23
24

25 It can be stated that there is a true lack of standardization of the material covering the human
26
27 skulls, not all materials are truly soft tissue equivalent, and some may even produce scatter
28
29 artefacts along the skull. Even more important with regard to pediatric dose optimization, is the
30
31 fact that age-specific pediatric skull phantoms are not commercially available. Thus, the aim of
32
33 the present report was to develop age-specific pediatric anthropomorphic head phantoms for
34
35 image quality and optimization studies, using Mix-D soft tissue equivalent material. The
36
37 subobjective was the validation of those resulting pediatric phantoms for image quality
38
39 assessment and optimization in the European DIMITRA project (*Dentomaxillofacial paediatric*
40
41 *imaging: an investigation towards low dose radiation induced risks*).
42
43
44
45
46
47

48 **Material and Methods**

49 *Natural skulls' features*

50
51 Six pediatric skulls were obtained with ethical approval from the anatomical collection of
52
53 Hasselt University (Hasselt, Belgium). The skulls were carefully selected based on age and
54
55 particular pathological characteristics. To that end, skulls were visually and radiographically
56
57
58
59
60
61
62
63
64
65

1
2
3
4 (panoramic radiographs) examined in order to estimate their ages according to the dental
5
6 development. Table 1 recaps the age estimation (from 4 to 10 years old) as well as particular
7
8 clinical and radiographic findings, allowing studies on diagnostic image quality.
9

10
11 All skulls were satisfactory preserved with regard to bone and dental tissues. Dental fractures
12
13 and cavities were observed by means of visual inspection, and then confirmed by radiographic
14
15 examinations. No large metallic restorations, dental posts or implants were present. Several
16
17 dental germs (normal or malpositioned), some missing teeth and a mesiodens were also
18
19 detected. Furthermore, one skull also presented internal and external dental resorptions in the
20
21 upper right central incisor and upper left lateral incisor (Figure 1).
22
23
24
25
26
27
28
29

30 *Soft tissue equivalent Mix-D preparation*

31
32 The Mix-D preparation was adapted from the study of Brand et al. 1989⁷, that described a
33
34 phantom for radiation dosimetry, using the original recipe introduced by Jones and Raine in
35
36 1949.¹⁵ For the present project, 500g of Mix-D was prepared in fractioned portions of 304g of
37
38 paraffin wax, 152g of polyethylene, 32g of magnesium oxide and 12g of titanium dioxide. First,
39
40 the wax, magnesium oxide and titanium dioxide were weighted, mixed and melted together
41
42 (105°C) in a glass round flask with a sufficient diameter to immerse the largest skull. When the
43
44 preparation was fully melted and mixed, polyethylene was added and the mixture heated for
45
46 another 20 minutes. The Mix-D manipulation procedure - preparation and skull covering - was
47
48 carried out in a fume hood to assure chemical safety.
49
50
51
52
53
54
55
56
57
58
59
60
61
62
63
64
65

1
2
3
4 *Skull covering*
5
6

7 Before the immersion process, skulls were protected with crepe tape (paper with adhesive
8 resin-rubber-based, 24mm width; 3M, Maplewood, MN, USA), especially in the areas of
9 foraminae (mandibular, mental, skull bases), large cavities (orbital, foramen magnum) and
10 teeth (Fig. 2A - B). This procedure avoids excessive infiltration of the melted material inside the
11 cranial cavities as well as through the interdental spaces.
12
13
14
15
16
17
18

19 For craniofacial covering, the skulls were held by the cranial bones and immersed in the melted
20 preparation up to the superior orbital arch (Fig. 2C). When the Mix-D presented the typical loss
21 of gloss indicating a pre-drying of the external surface, the skull was re-immersed. This
22 procedure was repeated several times until the achievement of a consistent and uniform layer
23 of Mix-D surrounding the skull. After 24 h, skulls were immersed in an inverted position,
24 holding them in the zygomatic arches areas. The mandibles were covered separately holding
25 the condyles and wrapped up to the cervical limit of the teeth (Fig. 2D). The inverted immersion
26 was also performed after 24 hours, in order to cover condyles, ramus and coronoid processes.
27
28
29
30
31
32
33
34
35
36
37
38
39
40
41
42
43
44
45
46
47
48
49
50
51
52
53
54
55

56 *CBCT scanning*
57
58

59 For validation purposes, the six resulting pediatric phantoms were scanned using two CBCT
60 units with different exposure parameter settings (CS9300, Carestream, Rochester, NY, USA and
61
62
63
64
65

1
2
3
4 NewTom Giano, *NewTom, Verona, Italy*). This allowed checking for artefact-free alignment of
5
6 the Mix-D onto the bony surface, with adequate thickness and homogeneous layering, thus
7
8 mimicking human soft tissues, as made visible on CBCT. Preliminary images deriving from all
9
10 scans were evaluated by 2 dentomaxillofacial radiologists, to check for air bubbles, artefacts
11
12 and inhomogeneity's of the Mix-D and a potential effect on the jaw bone. Only skulls presenting
13
14 perfect alignment of Mix-D surrounding the bone surfaces with adequate and realistic soft
15
16 tissue thickness density were accepted.
17
18
19
20
21

22 **Results**

23
24 Six DIMITRA pediatric phantoms (4 – 10 years old skulls) with Mix-D soft tissue equivalent
25
26 material have been prepared (figure 3); figure 4 allows a detailed view of phantom number 3.
27
28 Figure 5 shows a set of CBCT images obtained from the DIMITRA phantoms on the CS9300 unit
29
30 with large fields of view (17x11cm in A, B and C; 10x10cm in D, E and F). It is possible to note
31
32 the perfect alignment of the Mix-D surrounding the bone surfaces as well as the material
33
34 thickness and density compatible with the soft tissue aspect observed through *in vivo* CBCT
35
36 exams. There was a slight entry of melted Mix-D inside large bone cavities, mainly orbits,
37
38 maxillary sinus and nasal cavity. However, there were no gaps between Mix-D and bone
39
40 structures and resulting images were found mimicking clinical conditions.
41
42
43
44
45
46
47

48 Figure 6 allows a comparison between CBCT scans obtained from a DIMITRA phantom under
49
50 different exposure and reconstruction parameters (A, B and C) and from a child that presented
51
52 a clinical indication for a three-dimensional exam. The general similarity and close grey levels
53
54 of the Mix-D images (A-C) and the soft tissue aspect (D) can be noted. Other highlights include
55
56 the subjective visual differences related to noise and contrast patterns produced by different
57
58
59
60
61
62
63
64
65

1
2
3
4 CBCT units and technical parameters. Nevertheless, the perfect fit of the Mix-D to the bone
5
6 surfaces, following the outline and bone shape, seems to create favorable conditions for image
7
8 quality assessment.
9

10 11 **Discussion**

12
13
14 The presently introduced pediatric skull phantom collection has shown to be useful for age-
15
16 specific CBCT image quality assessment and optimization. In addition, the DIMITRA pediatric
17
18 phantoms showed some pathological conditions that might be useful for a number of imaging
19
20 studies, not only involving optimization, but also testing other experimental issues involving
21
22 two- and three-dimensional diagnostic imaging. The Mix-D preparation and embedding
23
24 technique described in the present report appears to be practical and reproducible, as long as
25
26 the right chemical proportion, melting sequence and immersion technique is used. On the
27
28 other hand, a drawback of the current technique is the difficulty to strictly control the thickness
29
30 of Mix-D during the layer-by layer immersion. As the melted material gets dry and solid, it is
31
32 difficult to introduce some measurement tool through the surface due to the risk of cracking.
33
34 This feature also becomes apparent when drilling slots for dosimeters insertion.⁷ However, for
35
36 image quality studies in which conventional dosimeters are not necessary, the present
37
38 phantoms are perfectly applicable. For instance, in the DIMITRA project, pediatric dosimetry
39
40 studies were performed using Monte Carlo simulation involving voxel phantoms; thus, there
41
42 was no need to construct slots for dosimeters.
43
44
45
46
47
48
49
50
51

52
53 Some infiltration of the Mix-D could be detected, especially in large cavities like orbits and
54
55 paranasal cavities. However, this material infiltration can be controlled and minimized by
56
57 means of protection with non-radiopaque tape. Furthermore, the specific Mix-D infiltration in
58
59
60
61
62
63
64
65

1
2
3
4 paranasal cavities may mimic some clinical pathological conditions like thickening of the sinus
5
6
7 membrane in allergic or inflammatory processes.
8

9
10 It is worth mentioning that, at this moment, we did not include natural cervical vertebrae and
11
12 soft tissues of the neck in the acquisitions, since matching pediatric vertebrae were not
13
14 available from the university's anatomical collection. Therefore, it can be expected that the
15
16 CBCT scans show a slight overestimation of the corresponding clinical image quality due to a
17
18 reduced X-ray attenuation from A-P and P-A projection angles as well as a reduced amount of
19
20 X-ray scatter, resulting in an increased signal-to-noise ratio at the level of the detector.
21
22
23 However, the use of the phantoms in (ongoing) follow-up studies involved the use of a
24
25 posterior support serving as a replacement for the neck, allowing for an evaluation of effects on
26
27 image quality in the presence and absence of neck tissue simulation.
28
29
30

31
32
33 Despite the aforementioned limitations with regard to development of age-specific pediatric
34
35 phantoms with soft tissue equivalent material, one should be aware that studies more closely
36
37 approaching clinical reality are ethically not tolerated. *In vivo* studies conducted with variations
38
39 of protocols and exposure factors are obviously not acceptable, especially for pediatric patients
40
41 considering their higher susceptibility to stochastic effects from radiation exposures.¹⁶ So, as
42
43 described above, the present phantoms are not a limitation-free model, but they represent a
44
45 starting point. Moreover, the soft tissue simulation method here described can be reproduced
46
47 and optimized from this first insight.
48
49
50

51
52
53 The phantoms are primarily intended for the evaluation of clinical image quality. To date, no
54
55 technical image quality parameters were measured for CBCT images of the DIMITRA phantoms
56
57
58 images such as contrast-to-noise ratio, modulation transfer function or CT number accuracy.
59
60
61
62
63
64
65

1
2
3
4 More studies involving objective measurements in the DIMITRA phantoms are necessary in
5
6
7 order to reinforce the preliminary subjective image quality results obtained up till now.
8

9
10 The rapidly changing field of CBCT technology urges the need for continuous monitoring of the
11
12 resulting image quality and related radiation doses. For this reason, further research is
13
14 continuously needed to allow optimization studies for clinical purposes. This may be of
15
16 particular interest when it comes to pediatric imaging.
17
18

19
20 In conclusion, the DIMITRA anthropomorphic phantoms developed by means the covering of six
21
22 pediatric skulls with Mix-D have shown appropriate images for dentomaxillofacial research
23
24 involving CBCT. Moreover, the layer-by-layer technique described here showed to be feasible to
25
26 perform, as long as all care and recommendations are follow strictly.
27
28

29 **Acknowledgments**

30
31
32 The research leading to these results has received funding from the European Atomic Energy
33
34 Community's Seventh Framework Programme FP7/2007–2011 under grant agreement no
35
36 604984 (OPERRA: Open Project for the European Radiation Research Area).
37
38
39
40
41
42

43 **REFERENCES**

- 44
45
46 1. Bushberg JT. Eleventh annual Warren K. Sinclair keynote address-science, radiation
47 protection and NCRP: building on the past, looking to the future. *Health Phys* 2015; 108:
48 115–23.
49
50
51 2. Oenning AC, Jacobs R, Pauwels R, Stradis A, Hedesiu M, Salmon B, DIMITRA Research
52 Group. Cone-beam CT in paediatric dentistry: DIMITRA project position statement.
53 *Pediatr Radiol* 2017; *in press*. (<https://doi.org/10.1007/s00247-017-4012-9>)
54
55
56
57
58 3. Farquharson MJ, Spyrou NM, al-Bahri J, Highgate DJ. Low energy photon attenuation
59 measurements of hydrophilic materials for tissue equivalent phantoms. *Appl Radiat Isot*
60
61
62
63
64
65

- 1
2
3
4 1995; 46: 783–90.
5
6
7 4. Nejjam Y, Silva AIV, Brasil DM, Vasconcelos KF, Haiter Neto F, Boscolo FN. Efficacy of lead
8 foil for reducing doses in the head and neck: a simulation study using digital intraoral
9 systems. *Dentomaxillofac Radiol* 2015; 44: 20150065.
10
11 5. Richards AG, Webber RL. Constructing phantom heads for radiation research. *Oral Surg*
12 *Oral Med Oral Pathol* 1963; 16: 683–90.
13
14 6. Hildebolt CF, Rupich RC, Vannier MW, Zerbolio DJ, Shrout MK, Cohen S, et al. Inter-
15 relationships between bone mineral content measures. *Dual energy radiography (DER)*
16 *and bitewing radiographs (BWV)*. *J Clin Periodontol* 1993; 20: 739–45.
17
18 7. Brand JW, Kuba RK, Braunreiter TC. An improved head-and-neck phantom for radiation
19 dosimetry. *Oral Surg Oral Med Oral Pathol* 1989; 67: 338–46.
20
21 8. Cook JE, Cunningham JL. The assessment of fracture healing using dual x-ray
22 absorptiometry: a feasibility study using phantoms. *Phys Med Biol* 1995; 40: 119–36.
23
24 9. Shelley AM, Brunton P, Horner K. Subjective image quality assessment of cross sectional
25 imaging methods for the symphyseal region of the mandible prior to dental implant
26 placement. *J Dent* 2011; 39: 764–70.
27
28 10. Melo SLS, Haiter Neto F, Correa LR, Scarfe WC, Farman AG. Comparative diagnostic yield
29 of cone beam CT reconstruction using various software programs on the detection of
30 vertical root fractures. *Dentomaxillofac Radiol* 2013; 42: 20120459.
31
32 11. Oliveira ML, Tosoni GM, Lindsey DH, Mendoza K, Tetradis S, Mallya SM. Influence of
33 anatomical location on CT numbers in cone beam computed tomography. *Oral Surg Oral*
34 *Med Oral Pathol Oral Radiol* 2013; 115: 558–64.
35
36 12. Lagos De Melo LP, Oenning ACC, Nadaes MR, Nejjam Y, Neves FS, Oliveira ML, et al.
37 Influence of Acquisition Parameters on the Evaluation of Mandibular Third Molars
38 Through Cone Beam Computed Tomography. *Oral Surg Oral Med Oral Pathol Oral Radiol*
39 2017.
40
41 13. Oliveira ML, Freitas DQ, Ambrosano GMB, Haiter Neto F. Influence of exposure factors on
42 the variability of CBCT voxel values: a phantom study. *Dentomaxillofac Radiol*; 2014; 43:
43 20140128.
44
45 14. Pauwels R, Jacobs R, Singer SR, Mupparapu M. CBCT-based bone quality assessment: are
46 Hounsfield units applicable? *Dentomaxillofac Radiol* 2015; 44: 20140238.
47
48 15. Jones DEA, Raine HC. Letter to the editor. *Br J Radiol*. 1949; 22: 549–50.
49
50 16. White SC, Scarfe WC, Schulze RKW, Lurie AG, Douglass JM, Farman AG, et al. The Image
51
52
53
54
55
56
57
58
59
60
61
62
63
64
65

1
2
3
4 Gently in Dentistry campaign: promotion of responsible use of maxillofacial radiology in
5 dentistry for children. Oral Surg Oral Med Oral Pathol Oral Radiol 2014; 118: 257–61.
6
7
8
9

10 **Figure Captions**

11
12 **Figure 1.** Panoramic reconstruction of skull 6. The white arrow indicates an internal resorption of
13 the root of the right central incisor and the black arrow points out an external root resorption
14 (apical third) of the left lateral incisor, possibly triggered by the deviation of the canine eruption
15 pathway.
16
17
18
19
20
21

22 **Figure 2.** The skulls were first covered with paper crepe-tape, mainly in the teeth and cavities,
23 in order to avoid overflowing of Mix-D (A, B). C and D show the “layer after layer” immersion
24 procedure for skulls and mandibles embedding, that took place in a round glass recipient, under
25 continuous low heating. A Mix-D tongue was also made (E-III) through a silicone model (E-I) and
26 an impression (E-II) that was filled up with melted Mix-D.
27
28
29
30
31
32

33 **Figure 3.** The six DIMITRA age-specific pediatric phantoms.
34
35
36
37

38 **Figure 4.** Phantom number 3, representing a child of 6 years old with the upper incisors in the
39 eruptive stage showing the first third of the crowns clinically.
40
41
42
43

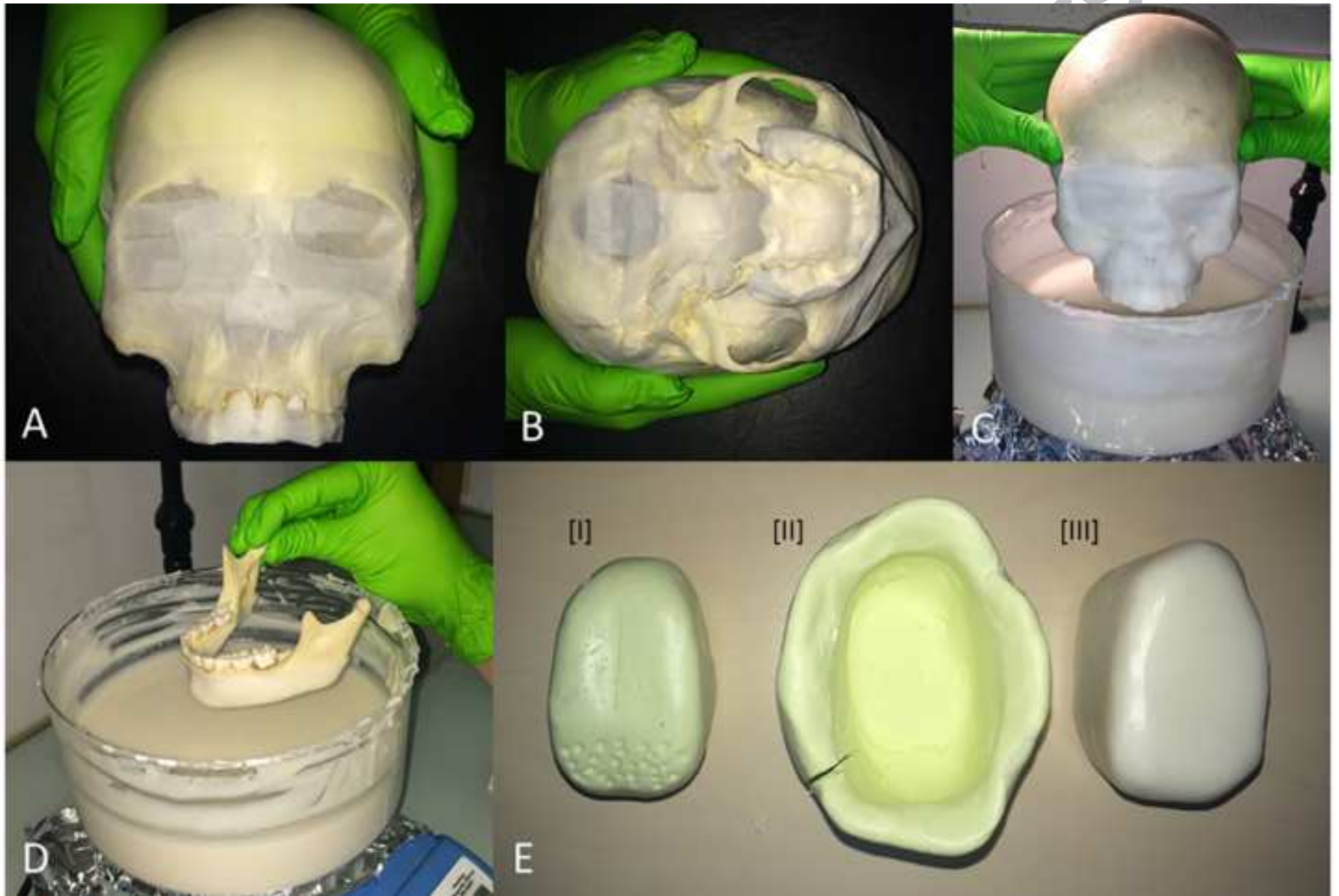
44 **Figure 5.** CBCT images obtained on the CS9300 unit, from phantoms 1 (A-C; field of view
45 17x11cm, 90 kV, 4mA, voxel size 0.3mm, 12 s) and 6 (D-E; A-C; field of view 10x10cm, 90 kV,
46 4mA, voxel size 0.18mm, 8 s). The images show a perfect fit of the Mix-D over the bone surfaces
47 and the smooth and continuous outline following the contour of the craniofacial structures. A
48 slight overflow of Mix-D can be detected inside the cranium (A- C), maxillary sinus (B, E),
49 sphenoid sinus (F), nasal cavity (B, C, E, F) and orbits (B, E). Axial (A, D) coronal (B, E) and sagittal
50 views (C, F).
51
52
53
54
55
56
57
58
59
60
61
62
63
64
65

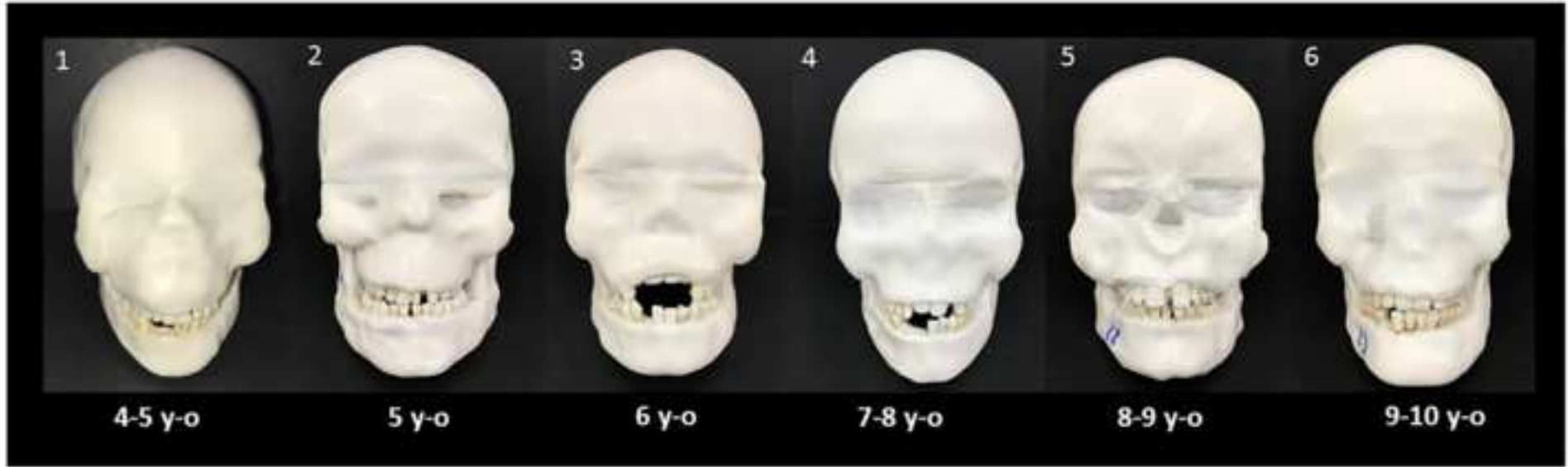
1
2
3
4 **Figure 6.** CBCT images of the DIMITRA phantom number 6, 9-10 years-old (A, B, C) and a 13
5 years-old boy (D) illustrating the similarity (soft tissue aspect) in different conditions (different
6 CBCT units and technical parameters). A: acquired from a CS9300 unit, FOV 5x5cm, 90kVp,
7 5mA, voxel size 0.09mm, 20s. B: acquired from a CS9300 unit, FOV 8x8cm, 90kVp, 5mA, voxel
8 size 0.18mm, 8s. C: acquired from a NewTom Giano unit, FOV 11x5cm, 90kVp, 3mA, voxel size
9 0.15mm, 9s. D: performed with a ProMax 3D Max unit (Planmeca, Helsinki, Finland), FOV
10 5x5cm, 96kVp, 11mA, voxel size 0.2mm, 12s (obtained from the clinical data collection of the
11 authors' institution).
12
13
14
15
16
17
18
19
20
21
22
23
24
25
26
27
28
29
30
31
32
33
34
35
36
37
38
39
40
41
42
43
44
45
46
47
48
49
50
51
52
53
54
55
56
57
58
59
60
61
62
63
64
65



DMFR

PROOFS



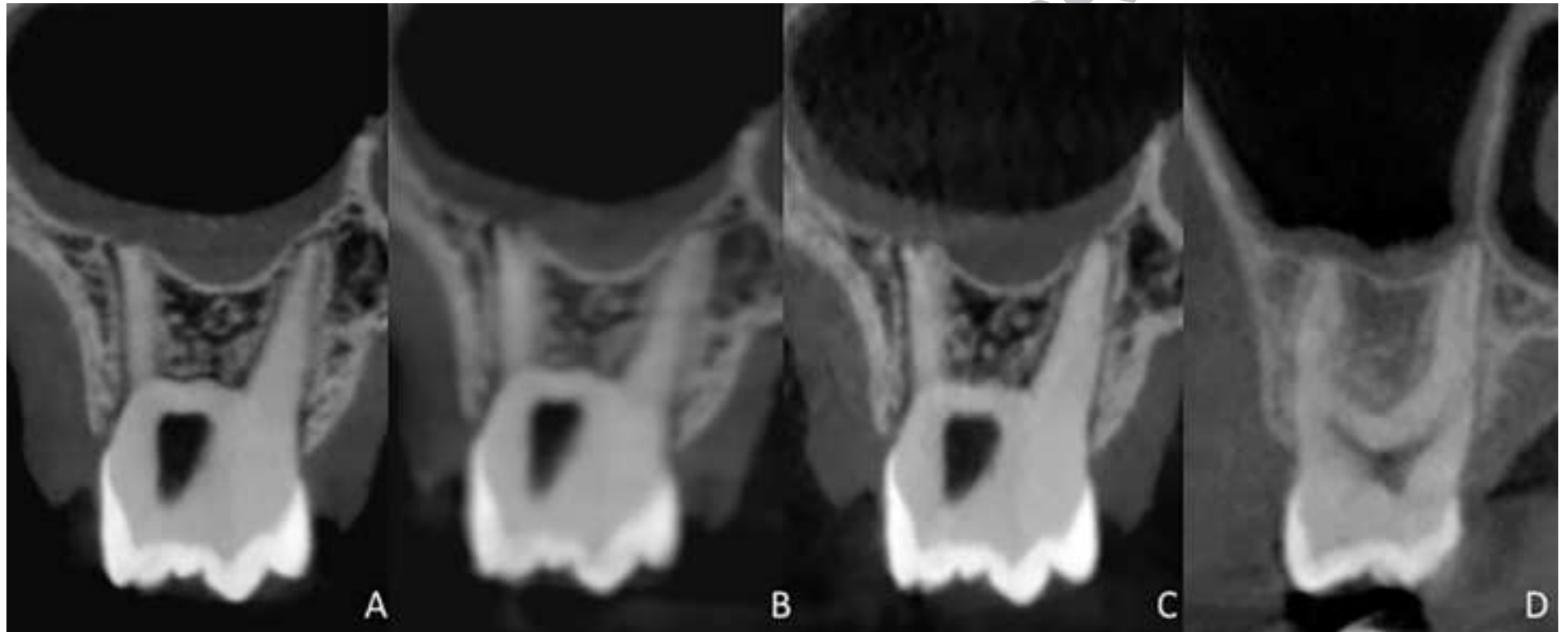


DMFR UA

PROOFS







DMFR

ROOFS

Table1. Age estimation of the skulls and the remarkable radiographic findings.

<i>Phantom</i>	<i>Age estimation</i>	<i>Radiographic findings</i>
1	4-5 years-old	Dental fractures, dental germs in malposition
2	5 years-old	Dental fractures, dental germs in malposition
3	6 years-old	Dental fractures
4	7-8 years-old	Dental fractures, missing teeth
5	8-9 years-old	Dental cracks, malposition of dental germs, mesiodens
6	9-10 years-old	Dental cracks, dental follicle enlargement, dental decay, root resorption (external and internal)

DMFR UNCORRECTED PROOFS